MOEM

Modern Electronic Materials 2022; 8(3): 97–105
DOI 10.3897/j.moem.8.3.97596

Research Article

Deep refinement of tellurium: equipment and process improvement through process simulation

Vladimir N. Abryutin[1], Igor I. Maronchuk[1], Nikolai A. Potolokov[1], Daria D. Sanikovich[1], Natalia I. Cherkashina[2]

1 ADV-Engineering, LLC, 3B 1st Lyusinovsky Lane, Moscow 119049, Russian Federation

2 Sevastopol State University, 33 Universitetskaya Str., Sevastopol 299053, Republic of Crimea

Corresponding author: Igor I. Maronchuk (igimar@mail.ru)

Received 8 September 2022 ♦ **Accepted** 26 September 2022 ♦ **Published** 14 October 2022

Citation: Abryutin VN, Maronchuk II, Potolokov NA, Sanikovich DD, Cherkashina NI (2022) Deep refinement of tellurium: equipment and process improvement through process simulation. *Modern Electronic Materials* 8(3): 97–105. https://doi.org/10.3897/j.moem.8.3.97596

Abstract

Simulation data have been presented on a process of deep refinement of tellurium based on Authors-developed refinement technique implemented through analysis of the process unit thermodynamical condition using Flow Simulation software, from SolidWorks software product. The technique put forward herein has been implemented in a plant comprising a vertical air-tight reaction chamber arranged inside a multi-zone thermal unit and executing a sequence of refinement stages which use different techniques and are integrated in a single process. The experimental data which have been the basis for calculations have allowed one to determine the boundary conditions of the mathematical model taking into account previous operation experience of the software product used. Temperature profile calculation has been carried out taking into account all the types of heat transfer in the system, the weight / dimensions parameters of system units and the physicochemical properties of refined tellurium, materials of equipment fittings and reactor media. The temperature modes of the process stages have been accepted as the boundary conditions for the thermal calculations, with temperatures being measured at equipment fitting locations at which temperature gages connected with a PID controller have been installed. The simulation of specific refinement process conditions allowed process modes and equipment fitting component design to be corrected. We have developed and produced test models of process and imitation equipment. Analysis of the thermal fields for the final model has shown good agreement with the mathematical model. Equipment upgrading and process parameter improvement on the basis of the simulation results have allowed T-u Grade tellurium (99.95 wt.%) refinement to a 99.99992 wt.% purity by 30 main impurities in the course of physical experiments, the product yield being at least 60%.

Keywords

tellurium, impurity composition, refinement techniques, filtration, vacuum distillation, mass spectroscopy, simulation

1. Introduction

High purity tellurium (Te) with a purity grade of 99,9999 wt.% (6N) or higher (6N+) finds wide application in electronics as a raw material for $A^{II}B^{VI}$ semiconductor compounds [1–4]. Achievement of good technical parameters for various instruments including RF devices and nuclear radiation detectors is impossible without the use of high-purity raw components including Te [5–8]. Major current manufacturers of high- and ultrahigh-purity materials including Cd, Zn and Te are 5N Plusinc. (Canada), Western Minметals Co. Ltd. (China), American Elements Inc. (US) which have the leading positions in the world market and deliver their products to Russian consumers, too [9]. The composition of impurities to be controlled and their concentration in Te are determined pursuant to the final semiconductor material requirements and intended use and are specified by the manufacturers. The continuous strengthening of the requirements to the degree of refinement which imminently entails complication of refinement processes and equipment used dictates the necessity of imposing limitations on the cost of high-purity raw materials. This is necessary for gaining competitive advantage and market attractiveness of respective products used for the design of high-efficiency devices in the fields of solar engineering, thermoelectric products and electronic components, as well as for stimulation of import substitution. Thus refinement process optimization is quite important for cost and labor consumption reduction in the high-tech industry.

The fabrication of Te with a purity of at least 6N+ includes a number of combined techniques on the basis of distillation processes [10–16], e.g. simple distillation implemented in one or multiple stages or multistage processes (rectification). The degree of refinement can be further increased using crystallization refinement techniques [17–20] which entail large operation expenses and require more complex equipment.

ADV-Engineering, LLC has for a long time optimized the process and equipment for high-purity Te on the basis of a distillation process (including a two-stage one) as the basic one, combined with various auxiliary operations including filtration, introduction of gettering impurities, refinement with refined element oxide as an impurity collector and vacuum degassing for solute gas removal. Special attention has been paid to studies of the role of process parameters (temperature of filtration, degassing, evaporation and fraction condensation processes, mass transport rates during volatile impurity removal and main material fraction distillation stages, shapes and dimensions of equipment components for optimum circulation of the gaseous and liquid phases etc.) [21, 22]. As a result a process has been developed that is implemented in a device having a vertical air-tight reactor arranged inside a multi-zone thermal unit and delivering a combination of sequential stages in a single process as described below [23].

1. Te melt filtration with simultaneous vacuum degassing and additional refinement by contacting with a refined element oxide layer, followed by transfer of molten material to the first distillation crucible.
2. First distillation during which the evaporating material is condensed in the area of the first distillation funnel.
3. Distillate drain to the second distillation crucible.
4. Melt degassing for removal of volatile impurities to the condenser in roughing vacuum (residual pressure above 0.001 Tor (1 Tor = 133.32 Pa)).
5. Second distillation in dynamic vacuum during which the evaporating refined material is condensed at the second distillation funnel.
6. Refined material drain and casting to consumer-specified weighed samples for further crystallization.

Tests of the process and experimental equipment developed herein allowed producing Te with the main component content of approx. 99.99985 wt.% from T-u Grade Te (99.95 wt.%) in a single process cycle without material reloading stages [23]. This result is superior to earlier ones achieved using separate process stages.

However in our opinion the technical capabilities of the process have not been exhausted yet. The aim of this work is to optimize the process that is currently used at ADV-Engineering, LLC by means of Te refinement process engineering aimed at achieving a main component content of at least 6N+ through correcting process modes and upgrading of equipment and fittings. Aiming at this task, thermal processes were simulated which take place in the vertical air-tight reactor arranged in the multi-zone unit with individual temperature control in each zone, and test experiments based on analysis of the simulation results and the quality of refined Te samples were carried out.

2. Process simulation

The thermal modes of the process and the design of the existing thermal unit comprising a reactor with graphite and quartz components of fittings were optimized through mathematical simulation of the Te refinement processes. The simulation was based on analysis of the thermodynamic condition of the thermal unit / reactor system in steady state mode at the start of each specific refinement stage. The working environment for the analysis was the FlowSimulation software from SolidWorks software product which delivers satisfactory calculation accuracy for the thermal process simulation task in question. The calculation was based on in-house work experience [21, 24, 25] (boundary conditions, thermal modes required for process stages) and specific known temperatures at the locations of controlling thermocouples connected to an OVEN TRM type PID temperature controller. The preset boundary conditions were used to calculate the temperature profiles in longitudinal and lateral cross-sections, the resultant temperature profiles

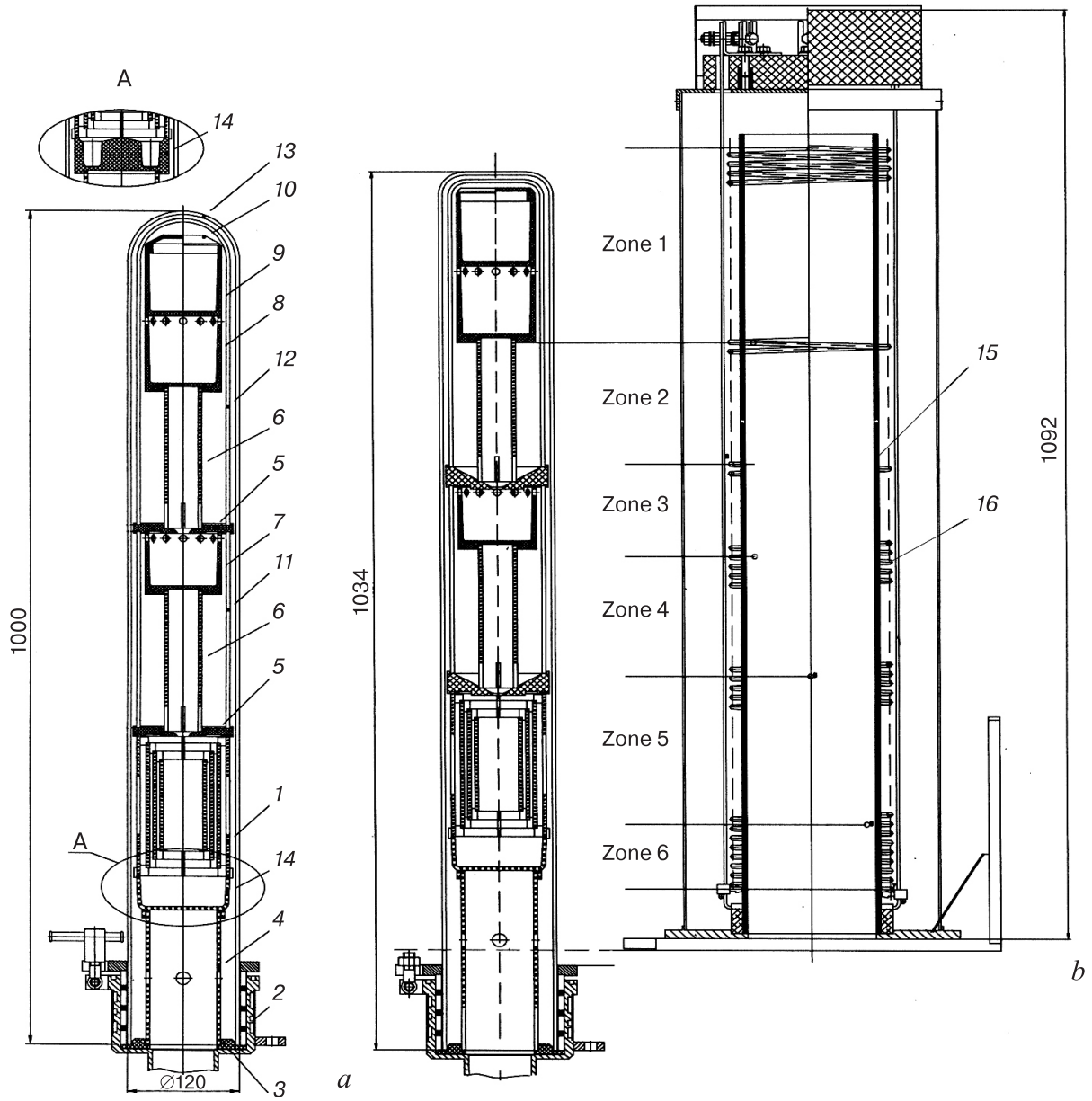

Figure 1. Reactor and fittings: *a*) initial design for optimization; *b*) upgraded design (left) for simulation and schematic diagram of furnace with heater zones (right) (*1* condenser; *2* gas and vacuum pipeline flange; *3* fluoroplastic lining; *4* input crucible support; *5* distillation funnel; *6* distillation crucible support; *7* second distillation crucible; *8* first distillation crucible; *9* loading crucible; *10* loading crucible cap; *11* distillation section poles; *12* distillation section flask; *13* quartz flask (reactor); *14* input crucible; *15* corundum muffle; *16* heaters)

were further compared with the experimentally derived thermal conditions and finally the reactor design was corrected (upgraded). The TRM PID controller temperature setting was corrected to deliver the optimum temperature profile for a process providing the maximum possible refinement degree and product output with a sufficient yield. The analysis was carried out taking into account the properties of the reactor and fittings materials and the working media.

The general appearance of the working equipment before and after upgrading and a schematic diagram of the thermal unit are presented in Fig. 1. It can be seen that the thermal unit comprises a heater with six independent heating zones delivering the possibility of setting the thermal profile parameters depending on the stage of the single process which includes the six operations described above.

Calculation of the first process stage (Te filtration) for the equipment design depicted in Fig. 1 *a* showed significant deviations of the resultant thermal profile from the optimum one reported earlier [19]. Selection of the required temperature mode for the first process stage entailed the need for following improvements to the reactor design:

– the height of the distillation crucible support was reduced and the length of the input crucible support was

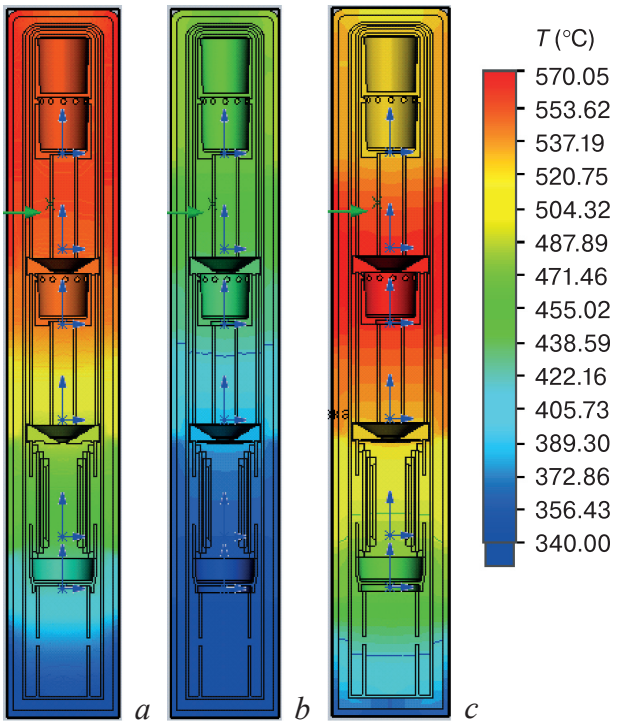

Figure 2. Simulated thermal field distribution along reactor with fittings: (*a*) filtration, (*b*) first distillation and (*c*) first drain

increased in order to provide for the required positions of the main reactor components (crucibles and condenser);

– the condenser length was increased in order to increase the efficiency of volatile component condensation;

– the overall reactor length was increased and the design of the top part of the reactor was optimized, along with the optimization of the input crucible cap and the distillation section flask, in order to change the length of the crucible supports;

– the design of the distillation funnels was changed substantially in order to reduce the radial temperature gradient and improve draining of the material.

Schematic diagram of the existing reactor design with fittings was corrected for calculations in order to optimize the design before passing on to the following process stages. The upgraded design of the reactor section with the new design of the nearby-located thermal unit comprising six heating zones is shown in Fig. 1 *b*. The heating zones are shown in Fig. 1 *b* relative to the reactor in a way they would be seen if the reactor was arranged in the full-sized thermal unit.

Thus the calculation of the first process stage allowed us to optimize the mathematical model, the thermal unit of the equipment and the design of the fittings and to avoid (minimize) the effect of negative parameters on the refinement process without carrying out numerous experiments or measurements. Further analytical work was carried out for the improved model wherein the device was arranged not in the thermal unit but in a corundum muffle (for calculation simplicity) which was divided into six heating zones as shown in Fig. 1 *b*.

The key process stages were simulated for the cases of empty fittings (without material) and with Te inside the fittings. Figures 2 and 3 show typical arrangements of heat fields throughout the process in a stage-wise manner for a single temperature range, from 340 to 570 °C. One can see temperature profiles both in the solid material and in the flowing media. The software used allows generating and measuring dynamic changes of temperature profiles for specific processes.

Figure 4 shows curves of axial temperature distributions for individual Te refinement process stages as shown in Figs. 2 and 3. The curves shown in Fig. 4 are in a good agreement with experimental thermal profile settings that were made before for all process stages [21, 23].

One can conclude that the equipment design and thermal profile settings can be calculated with a high accuracy thus tangibly reducing the labor consumption of preparation works for process development and startup. The above approaches can be used for equipment operation, e.g. after thermal unit replacement or after material changes (degradation) of the unit's electrical or thermal parameters.

Radial temperature cross-section profiles were studied at key locations of the fittings (e.g. at the distillation funnel for the distillation stage) for each process stage in order to determine the scatter of the temperature profiles in the lateral section of the system. The studies showed that the profile scatter in these sections is within 1 °C, i.e., there is no radial gradient. However, there are slight bends at the edges of the "plank" caused by the fact that

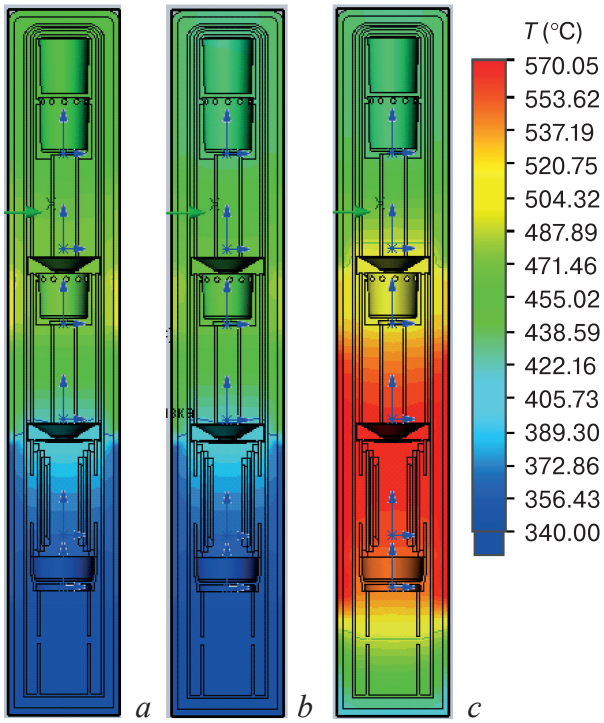

Figure 3. Simulated thermal field distribution along reactor with fittings: (*a*) vacuum degassing, (*b*) second distillation and (*c*) second drain

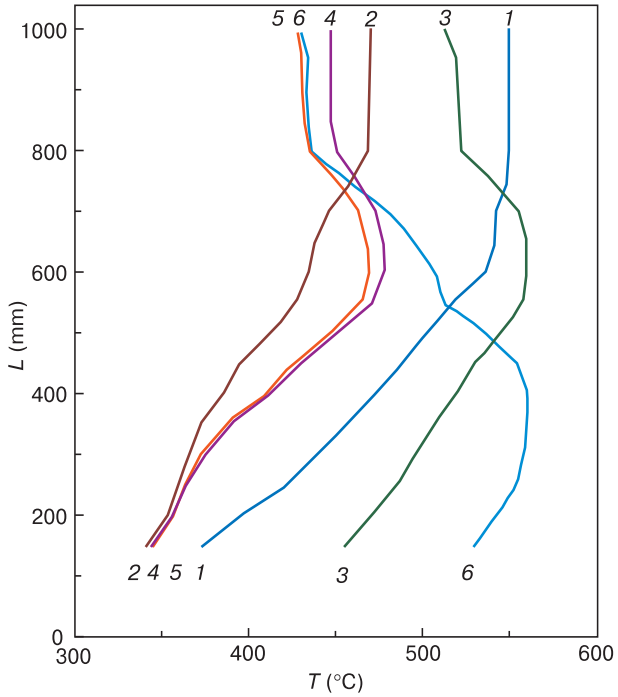

Figure 4. Axial temperature distributions for tellurium refinement process stages: (*1*) filtration, (*2*) first distillation, (*3*) first drain, (*4*) degassing, (*5*) second distillation and (*6*) second drain

the temperature in the muffle (heater) section is higher. However, this did not affect the quality of refinement.

It is of interest to calculate the effect of the introduction of refined material (Te) on the thermal conditions of the process. Figure 5 shows the distribution of temperature profiles across the reactor unit charged with Te in vacuum during second distillation and the axial temperature distribution in the reactor at that stage, in comparison with the axial temperature distribution under the same boundary conditions without the refined material. This process stage (second distillation) was chosen because the effect of the refined material in the reactor is the greatest at this stage since the refined material forms an additional shield at the second funnel thus strongly smoothening the temperature profile along the reactor axis above the funnel. Noteworthy, the presence of the refined material at these stages dramatically changes the pattern of the curves shown in Fig. 4 in the sections where the material is located. In this case there is an additional axial heat sink, i.e., heat radiation from the melt surface during distillation or from the surface of crystallized material collected at the funnel at an early stage of draining.

This situation, however, is not the case for the other process stages: the axial temperature distributions at the other process stages are almost similar for the empty reactor and for the reactor with refined material. This similarity shows itself primarily in the smoothening of the temperature front across the axis of graphite equipment components and therefore the introduction of a material having a lower or comparable heat conductivity affects the temperature profiles but slightly.

Depending on process stage, the calculations were carried out taking into account the presence or absence of a gas atmosphere with allowance for residual pressures that are required for the process. Analysis of gas flow dynamics in the reactor was carried out for different gas pressures. The temperature distribution along the gas flow was determined both for the gas media and for vacuum in the reactor cross-section, and deficiencies in the design of the reactor fittings that affect the gas flows in the reactor were identified. Some process openings (slots) in the quartz components of the fittings were redesigned (e.g. in the condenser, in the distillation crucible supports and in the input crucible support) in order to improve the process.

The calculations provided insight into the changes of the temperature fields at different stages throughout the whole process and allowed correcting the temperature modes for mass transport in different sections of the reactor unit and optimizing the temperature settings for the TRM controller as are required for the formation of temperature fields in the working zone during the entire sequence of process stages (Table 1).

3. Experimental

The experimental studies for mathematical simulation of the deep refinement process and the process equipment developed by the Authors included the following procedures:

– verification of agreement between the actual axial temperature profile in the reactor and the simulated profile;

Table 1. Recommended TRM controller temperature settings for Te refinement process stages

#	Process Stage	TRM temperature setting (°C)					
		Zone 1	Zone 2	Zone 3	Zone 4	Zone 5	Zone 6
1	Filtration	560.0	540.0	510.0	470.0	405.0	345.0
2	1st Distillation	470.0	450.0	430.0	400.0	360.0	355.0
3	1st Drain	530.0	570.0	568.0	540.0	500.0	480.0
4	Degassing	460.0	480.0	500.0	450.0	360.0	355.0
5	2nd Distillation	440.0	470.0	490.0	460.0	360.0	355.0
6	2nd Drain	350.0	470.0	520.0	570.0	570.0	568.0

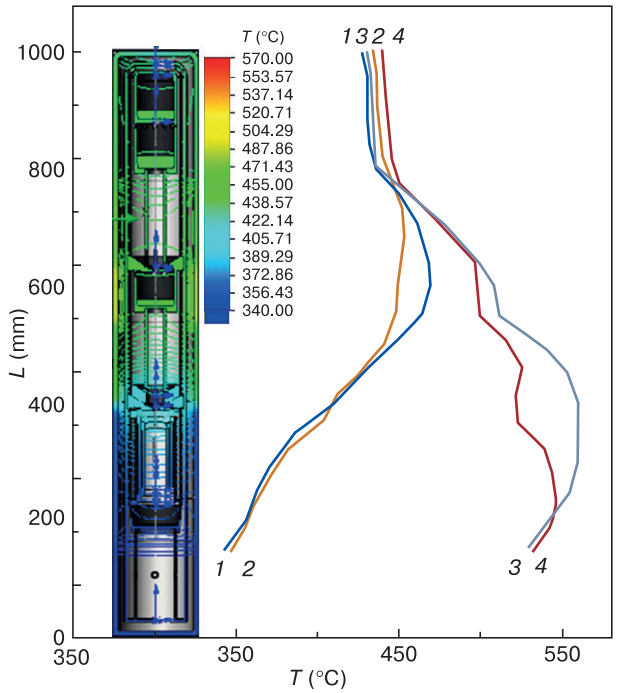

Figure 5. Temperature profile distribution in the reactor unit with material (Te) in vacuum during second distillation (left) and calculated axial temperature distribution in the reactor (right): (*1*) second distillation; (*2*) second distillation with tellurium; (*3*) second drain; (*4*) second drain with tellurium

- process testing with acquisition and analysis of technical and economic performance indicators of the process and the impurity composition of refined Te samples.

Imitating fittings were developed and fabricated for temperature measurement across the reactor axis inside the thermal unit. The fittings fully replicate the configuration of the standard reactor (Fig. 1 *b*) except that along the entire reactor there is a hollowed channel in the form of a quartz pipe. The channel has an inner diameter of 10 mm, and its top is soldered. The channel accommodates a type B thermocouple connected to an OVEN TRM101M metering device. After thermocouple installation the thermal unit was switched on with the controller temperature settings in accordance with the calculated and corrected temperature parameters for one of the six process stages obtained during process simulation (Table 1). The actual temperature profile was obtained by measuring the temperature at individual points by moving the thermocouple at a 10 mm step after the zone heaters reached a steady state mode (this was indicated by a metering device readings scatter of not greater than ±0.3 °C). The TRM temperature settings for different process stages were corrected during optimization based on specific process parameters [21, 23]. The experimentally selected temperature profiles for the reactor and the TRM temperature after correction are shown in Fig. 6 and in Table 2, respectively.

Comparison of the Te refinement process temperature profiles with those shown in Fig. 4 shows their good agreement. The difference between the simulated and the experimental temperatures in various sections of the curves is within 6 °C which is acceptable for the process in question. After all, one can make temperature corrections, typically minor ones, for any zone as required. This result confirms the correctness of the chosen approaches

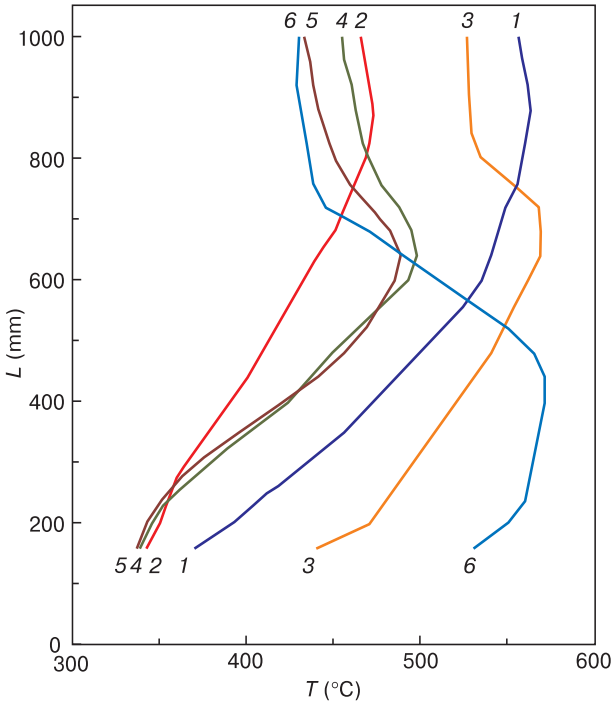

Figure 6. Axial temperature distribution in furnace unit for Te refinement stages: (*1*) filtration; (*2*) first distillation; (*3*) first drain; (*4*) degassing; (*5*) second distillation; (*6*) second drain

Table 2. Experimental TRM temperatures for Te refinement stages

#	Process Stage	TRM temperature setting (°C)					
		Zone 1	Zone 2	Zone 3	Zone 4	Zone 5	Zone 6
1	Filtration	565	548	515	470	405	345
2	1st Distillation	472	455	435	410	370	355
3	1st Drain	530	570	570	535	500	480
4	Degassing	460	485	495	448	360	355
5	2nd Distillation	445	467	490	455	380	355
6	2nd Drain	365	450	490	570	565	560

Table 3. Material balance for Te refinement process before and after equipment upgrading

#	Processes	Charge (g/%)	Residue (g/%)			Final product (g/%)	Loss (g/%)
			Loading crucible	First distillation crucible	Second distillation crucible	Input crucible	
1	Before upgrading	1800	181.8/10.1	340.2/18.9	271.8/15.1	995.4/55.3	10.8/0.6
2	After upgrading	1800	171.0/9.5	273.6/15.2	262.8/14.6	1081.8/60.1	10.8/0.6

Table 4. Elemental composition of Te samples taken at the initial, interim and final process stages

#	Impurity	Impurity content (wt.%)		
		T–u grade raw Te	Refined Te before upgrading [22]	Refined Te after upgrading
1	Ag	$2.57 \cdot 10^{-4}$	$<1 \cdot 10^{-6}$	$<1.20 \cdot 10^{-7}$
2	Sn	$<3.94 \cdot 10^{-6}$	$<3 \cdot 10^{-6}$	$<5.56 \cdot 10^{-7}$
3	Al	$9.3 \cdot 10^{-4}$	$6 \cdot 10^{-6}$	$<6.24 \cdot 10^{-6}$
4	Ti	$2.05 \cdot 10^{-6}$	$<3 \cdot 10^{-7}$	$<2.89 \cdot 10^{-6}$
5	P	—	$<1 \cdot 10^{-6}$	$<1.20 \cdot 10^{-6}$
6	B	$<3.55 \cdot 10^{-6}$	$<3 \cdot 10^{-6}$	$<3.59 \cdot 10^{-6}$
7	I	–	$<8 \cdot 10^{-7}$	$<8.00 \cdot 10^{-7}$
8	Ca	$3.78 \cdot 10^{-4}$	$<1 \cdot 10^{-6}$	$6.90 \cdot 10^{-6}$
9	Cu	$3.1 \cdot 10^{-3}$	$<1 \cdot 10^{-5}$	$<9.63 \cdot 10^{-7}$
10	Cr	$6.31 \cdot 10^{-5}$	$1 \cdot 10^{-6}$	$<3.08 \cdot 10^{-7}$
11	Fe	$1.81 \cdot 10^{-4}$	$5 \cdot 10^{-6}$	$<2.88 \cdot 10^{-6}$
12	In	$3.37 \cdot 10^{-5}$	$1 \cdot 10^{-6}$	$<9.06 \cdot 10^{-9}$
13	Mg	$<3.51 \cdot 10^{-6}$	$<3 \cdot 10^{-7}$	$<7.76 \cdot 10^{-6}$
14	Mn	$6.31 \cdot 10^{-6}$	$2 \cdot 10^{-6}$	$<5.00 \cdot 10^{-7}$
15	Mo	$<4.98 \cdot 10^{-5}$	$<2 \cdot 10^{-6}$	$<7.74 \cdot 10^{-7}$
16	Ni	$<4.93 \cdot 10^{-6}$	$1 \cdot 10^{-6}$	$<5.19 \cdot 10^{-7}$
17	Pb	$1.66 \cdot 10^{-3}$	$<6 \cdot 10^{-6}$	$<1.20 \cdot 10^{-6}$
18	Tl	$3.99 \cdot 10^{-4}$	$<6 \cdot 10^{-6}$	$<7.24 \cdot 10^{-7}$
19	Cl	—	$2 \cdot 10^{-6}$	$2.00 \cdot 10^{-6}$
20	Co	$9.68 \cdot 10^{-6}$	$1 \cdot 10^{-6}$	$<2.43 \cdot 10^{-7}$
21	Sb	$4.63 \cdot 10^{-6}$	$<1 \cdot 10^{-5}$	$2.66 \cdot 10^{-6}$
22	Na	$3.8 \cdot 10^{-3}$	$<1 \cdot 10^{-6}$	$<5.52 \cdot 10^{-6}$
23	Si	$1.8 \cdot 10^{-3}$	$5 \cdot 10^{-5}$	$1.71 \cdot 10^{-5}$
24	K	$2.78 \cdot 10^{-5}$	$<1 \cdot 10^{-6}$	$<3.07 \cdot 10^{-6}$
25	V	$9.64 \cdot 10^{-7}$	$<3 \cdot 10^{-7}$	$<1.32 \cdot 10^{-6}$
26	Li	$<1.02 \cdot 10^{-6}$	$<1 \cdot 10^{-6}$	$<8.76 \cdot 10^{-7}$
27	Cd	$3.91 \cdot 10^{-3}$	$<2 \cdot 10^{-7}$	$<4.97 \cdot 10^{-6}$
28	Zn	$<4.67 \cdot 10^{-5}$	$6 \cdot 10^{-6}$	$<2.53 \cdot 10^{-6}$
29	As	$<3.13 \cdot 10^{-6}$	$2 \cdot 10^{-6}$	$<8.31 \cdot 10^{-7}$
30	Se	$9.05 \cdot 10^{-5}$	$2 \cdot 10^{-5}$	$<6.14 \cdot 10^{-7}$
31	S	—	$<1 \cdot 10^{-6}$	$<1.00 \cdot 10^{-6}$
Main material		99.98	99.99985	99.99992
Total impurities		0.02	0.00015	0.00008
Refinement degree		—	133	250

to the development of a combined Te refinement process and equipment for its implementation.

The TRM temperature settings (Tables 1 and 2) for these profiles (Figs. 4 and 6) differ significantly, presumably due to the different installation locations of the control thermocouples in the thermal unit. For theoretical calculations the thermocouple installation locations were chosen to be at the muffle of the furnace where in the actual thermal unit the thermocouples were installed between heater coils in the middle of the heating zones.

Tellurium refinement tests were carried out on the basis of the data obtained,. The raw material was T-u Grade Te (99.95 wt.%) produced in accordance with the TU 20.13.21-096-00194429-2020 Technical Conditions of a Russian manufacturer. An 1800 g weighed sample for refinement was cleaved from raw material ingots.

Combined fittings were used for refinement, part of the fittings being made from MPG-7 Grade graphite produced in accordance with the TU 1915-051-002008510 2005 Technical Conditions of a Russian manufacturer (Fig. 1, *5*, *7—10*, *14*), and the other from fused silica pipes produced in accordance with the Russian State Standard GOST 15177-70. Maximum possible purity was achieved by treating the graphite and quartz components before loading in accordance with the in-house technique (graphite components were air-annealed at a residual pressure of max. 0.00001 mm Hg and quartz components were treated with a mixture of mineral acids, degreased, dried and annealed under the same conditions as above).

4. Results and discussion

Upon the completion of test Te refinement experiments with the upgraded plant the reactor was opened and unloaded, and the crucible residue, the final product and the condensate were weighed. Table 3 shows data on averaged material balance for the Te refinement process before [22] and after equipment upgrading.

Test samples of the material were taken at the input QC and from the final product. The samples were analyzed at the Giredmet Test Center by spark mass spectrometry on a JMS-01-BM2 double-focus mass spectrometer (JEOL) and independently at ARMOLED Co. on a NexION induction coupled plasma mass spectrometer. The results for the raw material before and after equipment upgrading are summarized in table 4. It should be noted that raw tellurium was T-u Grade taken from a single batch. The overall impurity content was calculated taking into account the detection thresholds of metering equipment for specific impurities. Table 4 shows the impurity composition for the impurities considered as functional ones (in accordance with literary data [2, 3, 26, 27]) for the growth of CdZnTe and CdTe crystals used in the fabrication of ionizing radiation detectors.

5. Conclusion

Deep tellurium refinement processes based on an earlier developed technique were simulated by analyzing the thermodynamic condition of the thermal unit / reactor system using the Flow Simulation software from SolidWorks software product. The simulation results allowed us to made fundamental changes to technical approaches used in the tellurium refinement process and to upgrade process equipment for developing the optimum conditions at all refinement stages. A test model of process fittings and imitation fittings for thermal field measurement were developed and fabricated, providing for experimental verification of agreement with mathematical simulation results. Physical T-u Grade Te (99.95 wt.%) refinement experiments showed the possibility of obtaining material with a main component content of 99.99992 wt.% by 30 basic impurities with a final product yield of above 60%. This is superior to the results obtained before equipment upgrading (the overall impurity content is reduced by 1.9 times and the yield is increased by 1.09 times) thus confirming the correctness of the technical solutions chosen.

Acknowledgement

This study was funded by the Innovation Support Foundation, Project No. 63431.

References

1. Azhazha V.M., V'yugov P.N., Kovtun G.P., Neklyudov I.M. Production and use of some high-purity rare metals. *Problems of Atomic Science and Technology. Series: Vacuum, pure materials, superconductors*. 2004; (6(14)): 3–6. (In Russ.). http://dspace.nbuv.gov.ua/bitstream/handle/123456789/81248/01-Azhazha.pdf
2. Kovtun G.P., Kondrik A.I. Investigation of the properties of semiconductor materials for detectors of ionizing radiation. *Tekhnologiya i Konstruirovanie v Elektronnoi Apparature*. 2003; (6): 3–6. (In Russ.). http://dspace.nbuv.gov.ua/bitstream/handle/123456789/70708/01-Condrik.pdf
3. Kondrik A.I., Kovtun G.P. Influence of impurities and structural defects on electrophysical and detector properties of CdTe and CdZnTe. *Tekhnologiya i Konstruirovanie v Elektronnoi Apparature*. 2019; (5-6): 43–50. (In Russ.). https://doi.org/10.15222/TKEA2019.5-6.43
4. Shcherban' A.P., Kovtun G.P. Obtaining high purity cadmium for microelectronics. *Visnyk of V.N. Karazin Kharkiv National University. Physical series "Nuclei, particles, fields"*. 2004; (642(3(25))): 27–34. (In Russ.). http://nuclear.univer.kharkov.ua/lib/642_3(25)_04_p27-34.pdf

5. Gribov B.G. Critical materials of electronic engineering. In: *High-purity substances and materials. Obtaining, analysis, application. Abstracts XII Conf.* Nizhnii Novgorod, May 31 – June 3, 2004. Nizhnii Novgorod: Izdatel' Yu.A. Nikolaev; 2004: 4–6. (In Russ.)
6. Kovtun G.P., Kravchenko A.I., Shcherban' A.P. Production of high-purity gallium, zinc, cadmium and tellurium for microelectronics. *Tekhnologiya i Konstruirovanie v Elektronnoi Apparature.* 2001; (3): 6–8. (In Russ.)
7. Azhazha V.M., Kovtun G.P., Neklyudov I.M. An integrated approach to obtaining high-purity materials for electronics. *Tekhnologiya i Konstruirovanie v Elektronnoi Apparature.* 2002; (6): 3–6. (In Russ.)
8. Churbanova M.F., Karpova Yu.A., Zlomanova P.V., Fedorov V.A., eds. High-purity substances. Moscow: Nauchnyi mir; 2018. 994 p. (In Russ.). https://www.elibrary.ru/fjftev
9. Kul'chitskii N.A., Naumov A.V. State of markets of cadmium, tellurium, and related compounds. *Izvestiya. Non-Ferrous Metallurgy*. 2010; (6): 58–65. (In Russ.). https://www.elibrary.ru/nbhycr
10. Kozin L.F., Berezhnoi E.O., Kozin K.L. Patterns of deep purification of cadmium by distillation. *Vysokochistye Veshchestva*. 1996; (5): 11–29. (In Russ.)
11. Kalashnik O.N., Nisel'son N.A. Purification of simple substances by distillation with hydrothermal oxidation of impurities. *Vysokochistye Veshchestva*. 1987; (2): 74–78. (In Russ.)
12. Shcherban A.P., Kovtun G.P., Gorbenko Y.V., Solopikhin D.A., Virich V.D., Pirozhenko L.A. Production of high purity granular metals: cadmium, zinc, lead. *Tekhnologiya i Konstruirovanie v Elektronnoi Apparature.* 2017; (1-2): 55–60. (In Russ.). https://doi.org/10.15222/TKEA2017.1-2.55
13. Patent (RU) No. 2687403, IPCC01B 19/02, C22B 9/04. Grishechkin M.B., Khomyakov A.V., Mozhevitina E.N., Avetisov I.Kh. Method for producing high-purity tellure by distillation with low content of selenium. Appl.: 08.10.2018, publ.: 13.05.2019. (In Russ.). https://yandex.ru/patents/doc/RU2687403C1_20190513
14. Grishechkin M.B. Application of gas-phase technologies for deep purification of substances based on rare elements. Diss. Cand. Sci. (Chem.). Moscow; 2021. 256 p. (In Russ.). http://www.irea.org.ru/education/dissertation-council/Диссертация_Гришечкин_ФИН.pdf
15. Aleksandrov B.N., D'yakov I.G. Purification of technical cadmium by vacuum distillation using a heated condenser. *The Physics of Metals and Metallography.* 1962; 14(4): 569–573. (In Russ.)
16. Grishechkin M.B., Mozhevitina E.N., Khomyakov A.V., Zykova M.P., Avetisov R.I., Avetissov I.C. Deep tellurium purification for electronic and photonic materials. *Izvestiya Vysshikh Uchebnykh Zavedenii. Materialy Elektronnoi Tekhniki = Materials of Electronics Engineering*. 2016; 19(4): 235–240. (In Russ.). https://doi.org/10.17073/1609-3577-2016-4-235-240
17. Potolokov N.A., Fedorov V.A. Ultrapurification of tellurium and cadmium by distillation and crystallization. *Inorganic Materials*. 2012; 48(11): 1082–1087. https://doi.org/10.1134/S0020168512110106
18. Pfann G. Zone melting. NY: Wiley; London: Chapman and Hall; 1960. 272 p. (Russ. Transl.: Pfann V. Zonnaya plavka. Moscow: Metallurizdat; 1960. 272 p.)
19. Aleksandrov B.N., Verkin B.I. Purification of electrolytically pure cadmium by zone recrystallization and vacuum distillation. *The Physics of Metals and Metallography.* 1960; 9(3): 362–365. (In Russ.)
20. Shcherban' A.P., Kovtun G.P., Datsenko O.A. Classification of the behavior of impurities in zinc, cadmium and tellurium during crystallization purification. *Problems of Atomic Science and Technology. Series: Vacuum, pure materials, superconductors*.2004; (6): 16–20. (In Russ.). http://dspace.nbuv.gov.ua/bitstream/handle/123456789/81250/03-Kovtun.pdf?sequence=1
21. Patent (RU) No. 2777064, IPC C01B 19/02, C22B 9/04. Davydova E.V., Egorov M.A., Maronchuk I.I., Sanikovich D.D. Method for deep cleaning of metals. Appl.: 17.06.2021; publ.: 22.07.2022. (In Russ.). https://patentimages.storage.googleapis.com/2e/e4/28/125c8a932942fa/RU2776574C1.pdf
22. Patent (RU) No. 2777064, IPC C01B 19/02, C22B 9/04, C22B 9/02. Davydova E.V., Egorov M.A., Maronchuk I.I., Sanikovich D.D. Apparatus for deep purification of metals Davydova E.V., Egorov M.A., Maronchuk I.I., Sanikovich D.D. Appl.: 17.06.2021; publ.: 01.08.2022. (In Russ.). https://patentimages.storage.googleapis.com/87/58/10/12c6a34b7e8f24/RU2777064C1.pdf
23. Abryutin V.N., Davydova E.V., Egorov M.A., Maronchuk I.I., Sanikovich D.D. Deep purification of tellurium, zinc and cadmium for electronic applications. *Izvestiya Vysshikh Uchebnykh Zavedenii. Materialy Elektronnoi Tekhnikii = Materials of Electronics Engineering.* 2022; 25(2): 164–174. (In Russ.). https://doi.org/10.17073/1609-3577-2022-2-164-174
24. Maronchuk I.I., Sanikovich D.D., Potapkov P.V., Vel′chenko A.A. Improvement of the processes of liquid-phase epitaxial growth of nanoheteroepitaxial structures. *Journal of Engineering Physics and Thermophysics.* 2018; 91(2): 491–497. https://doi.org/10.1007/s10891-018-1769-0
25. Maronchuk I.I., Sanikovitch D.D., Cherkashin A.S., Nitchev H., Dimova-Malinovska D. Improving the growth of Ge quantum dots by liquid-phase epitaxy. *Journal of Physics: Conference Series*. 2017; (794): 012012. https://doi.org/10.1088/1742-6596/794/1/012012
26. Zazvorka J., Hlidek P., Franc J., Pekarek J., Grill R. Photoluminescence study of surface treatment effects on detector-grade CT: In. *Semiconductor Science and Technology.* 2016; 31(2): 250–258. https://doi.org/10.1088/0268-1242/31/2/025014
27. Zázvorka J. Doctoral thesis, photoconductivity, photoluminescence and charge collection in semiinsulating CT and CZT. Prague: Institute of Physics of Charles University; 2016. 49 p. https://dspace.cuni.cz/handle/20.500.11956/82430